Jurnal Teknologi

Full paper

# Mooring Effect on Wave Frequency Response of Round Shape FPSO

C. L. Siow[a], J. Koto[a,b*], H. Yasukawa[c], A. Matsuda[d], D. Terada[d], C. Guedes Soares[e], Atilla Incecik[f], Pauzi M. A. G.[a]

[a]*Department of Aeronautics, Automotive and Ocean Engineering, Faculty of Mechanical Engineering, Universiti Teknologi Malaysia, 81310 UTM Johor Bahru, Johor, Malaysia*
[b]*Ocean and Aerospace Research Institute, Indonesia*
[c]*Department of Transportation and Environmental Systems, Hiroshima University, Japan*
[d]*National Research Institute of Fisheries Engineering (NRIFE), Japan*
[e]*Centre for Marine Technology and Engineering (CENTEC), Instituto Superior Técnico, Universidade de Lisboa, Portugal*
[f]*Department of Naval Architecture, Ocean and Marine Engineering, University of Strathclyde, Glasgow, United Kingdom*

*Corresponding author: jaswar@mail.fkm.utm.my and jaswar.koto@gmail.com

**Article history**

Received :25 December 2014
Received in revised form :
25 March 2015
Accepted :15 May 2015

**Graphical abstract**

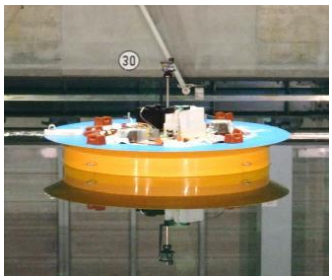

**Abstract**

This paper presents the motions response of moored Round Shape FPSO model due to the wave effect. The proposed of this research is analyzed the possibility of model motion response affected by different mooring system attach to the model. Model experiment was applied in this research to collect motion data for the study. Besides, the numerical simulation using diffraction potential, diffraction potential with Morison Heave correction and ANSYS frequency domain study were also applied in this research to generate comparative data to the experimental results. To investigate the effect of the mooring system to motion response, the model experiment was firstly conducted by attached model scale catenary mooring lines to Round Shape FPSO model. After that, the experiment was repeated by attached model scale taut mooring lines to the same model. The results obtain from the regular wave experiment tests and numerical simulation test were presented in this paper. This research concluded that the mooring systems would not give significant effect to wave frequency motion response after compared the motion result obtain from model experiment conducted using different mooring system.

*Keywords*: Round Shape FPSO; wave response; diffraction potential; damping correction, motion test; mooring



## 1.0 INTRODUCTION

Deep water oil and gas exploration is a costly industry activity due to the required of high technology level during exploration. In deep water region, floating structures is more comparative compare to the fix structure. To control the movement of floating structure, mooring system is used if the water depth is within reasonable depth. Generally, two types of mooring system available, there are catenary mooring and taut mooring. Both of the mooring system frequently use in offshore industry to control the movement of the floating structures.

Besides, a lot of Floating Production Storage and Offloading, FPSO structures are converted from an old tanker ships but some of the FPSO owners are interest for new constructed hulls. In term of system requirement, the FPSO require better performance in stability either static or dynamic condition compare to resistance performance. The different of operation requirement causes related industry to develop new generation FPSO with more practical hull form for the offshore desire.

In year 2008, Lamport and Josefsson, (2008) carried a research to study the advantage of round shape FPSO over the traditional ship-shape FPSO [1]. The comparisons were made to compare motion response, mooring system design, constructability and fabrication, operability, safety and costing between both the structures. One of the finding on their study is the motions of their designed structures are similar at any direction of incident wave with little yaw excitation due to mooring and riser asymmetry. Next, Arslan, Pettersen, and Andersson (2011) are also performed a study on fluid flow around the round shape FPSO in side-by-side offloading condition. FLUENT software was used to simulate three dimensional (3D) unsteady cross flow pass a pair of ships sections in close proximity and the behavior of the vortex-shedding around the two bluff bodies [2]. Besides, simulation of fluid flow Characteristic around Rounded-Shape FPSO by self-develop programming code based on RANs method also conducted by A. Efi *et al*. [3].

To study the wave motion response of FPSO, diffraction potential method is used frequently and the accuracy of this method to predict the structures response was also detailed studied. The diffraction potential theory estimates wave exciting forces on the floating body based on the frequency domain and this method can be considered as an efficient one to study the motion of large size

floating structure with acceptable accuracy. The good accuracy of this diffraction theory applied to large structures is due to the significant diffraction effect that exists in the large size structure in wave [4].

In this study, the motion response of a Round Shape FPSO is simulated by self-developed programming code based on diffraction potential theory with Morison damping correction method. The accuracy of this programming code was checked with the previous semi-submersible experiment result which carried out at the towing tank belong to Universiti Teknologi Malaysia [5]. A theoretical review on these diffraction potential theory and diffraction potential with Morison drag correction method were conducted. The reviews simulate the motion response of Round Shape obtained from the proposed methods and compared the tendency of the simulation results [9].

In this paper, the effect of mooring to the FPSO motion response was studied by experimental method. The wave motion experiment was conducted by attached the model scale catenary mooring to the Round FPSO and then the same test was repeated by replace the model scale catenary mooring with taut mooring so the experiment can capture the wave frequency motion and slow drifts motion. These wave tank experiments were conducted by C. L. Siow *et al.* in regular wave condition to the designed Round FPSO model in scale 1:110 [6]. The mooring design was conducted before the experiment so the suitable mooring line was selected to achieve the experiment target [7]. In this paper, the main discussions are focused in the effect of difference mooring system to the motion of Round Shape FPSO. The motion experiments results collected by fixed the FPSO with catenary mooring and taut mooring are compared with simulation result too. The comparison showed that the simulation results were validated by both the motions experiment result collected when the model was fixed with catenary mooring and taut mooring because the experiments results do not show significant effect of different mooring system to wave frequency motion.

## ■2.0 NUMERICAL CALCULATION

### 2.1 Diffraction Potential

In this study, the diffraction potential method was used to obtain the wave force act on the Round Shape FPSO also the added mass and damping for all six directions of motions. The regular wave acting on floating bodies can be described by velocity potential. The velocity potential normally written in respective to the flow direction and time as below:

$$\Phi(x,y,z) = Re\left[\phi(x,y,z)e^{iwt}\right] \tag{1}$$

$$\phi(x,y,z) = \frac{g\varsigma_a}{iw}\{\phi_0(x,y,z) + \phi_7(x,y,z)\} + \sum_{j=1}^{6} iwX_j\phi_j(x,y,z) \tag{2}$$

where,

g : Gravity acceleration
$\varsigma_a$ : Incident wave amplitude
$X_j$ : Motions amplitude
$\phi_0$ : Incident wave potential
$\phi_7$ : Scattering wave potential
$\phi_j$ : Radiation wave potential due to motions
$j$ : Direction of motion

From the above equation, it is shown that total wave potential in the system is contributed by the potential of the incident wave, scattering wave and radiation wave. In addition, the phase and amplitude of both the incident wave and scattering wave are assumed to be the same. However, radiation wave potentials are affected by each type of motions of each single floating body in the system, where the total radiation wave potential from the single body is the summation of the radiation wave generates by each type of body motions such as surge, sway, heave, roll, pitch and yaw,

Also, the wave potential $\emptyset$ must be satisfied with boundary conditions as below:

$$\nabla^2\emptyset = 0 \quad for\ 0 \le z \le h \tag{3}$$

$$\frac{\partial\emptyset}{\partial z} + k\emptyset \quad at\ z = 0 \quad \left(k = \frac{w^2}{g}\right) \tag{4}$$

$$\frac{\partial\emptyset}{\partial z} = 0 \quad at\ z = h \tag{5}$$

$$\emptyset \sim \frac{1}{\sqrt{r}}e^{-ik_0 r} \quad should\ be\ 0\ if\ r\ \infty \tag{6}$$

$$\frac{\partial\phi_7}{\partial n} = -\frac{\partial\emptyset_0}{\partial n}\ on\ the\ body\ boundary \tag{7}$$

### 2.2 Wave Potential

By considering the wave potential only affected by model surface, $S_H$, the wave potential at any point can be presented by the following equation:

$$\emptyset(P) = \iint_{S_H}\left\{\frac{\partial\emptyset(Q)}{\partial n_Q}G(P;Q) - \emptyset(Q)\frac{\partial G(P;Q)}{\partial n_Q}\right\}dS(Q) \tag{8}$$

Where $P$ =($x$, $y$, $z$) represents fluid flow pointed at any coordinate and $Q = (\xi,\eta,\varsigma)$ represent any coordinate, ($x$, $y$, $z$) on model surface, $S_H$. The green function can be applied here to estimate the strength of the wave flow potential. The green function in eq. (8) can be summarized as follow:

$$G(P;Q) = -\frac{1}{4\pi\sqrt{(x-\xi)^2+(y-\eta)^2+(z-\zeta)^2}} + H(x-\xi,y-\eta,z+\zeta) \tag{9}$$

where $H(x-\xi,y-\eta,z+\zeta)$ in eq. (9) represent the effect of free surface and can be solved by second kind of Bessel function.

### 2.3 Wave Force, Added Mass and Damping

The wave force or moment act on the model to cause the motions of structure can be obtained by integral the diffraction wave potential along the structure surface.

$$E_i = -\iint_{S_H} \phi_D(x,y,z) n_i dS \quad (10)$$

where, $\phi_D$ is diffraction potential, $\phi_D = \phi_o + \phi_7$

Also, the added mass, $A_{ij}$ and damping, $B_{ij}$ for each motion can be obtained by integral the radiation wave due to each motion along the structure surface.

$$A_{ij} = -\rho \iint_{S_H} Re[\phi_j(x,y,z)] n_i dS \quad (11)$$

$$B_{ij} = -\rho w \iint_{S_H} Im[\phi_j(x,y,z)] n_i dS \quad (12)$$

$n_i$ in eq. (10) to eq. (12) is the normal vector of each direction of motion, $i$ = 1~ 6 represent the direction of motion and $j$ = 1~6 represent the six type of motions

### 2.4 Drag Term of Morison Equation

The linear drag term due to the wave effect on submerge model is calculated using Drag force equation as given by Morison equation:

$$F_D = \frac{1}{2}\rho A_{Proj} C_D |\dot{\phi}_Z - \dot{X}_z|(\dot{\phi}_Z - \dot{X}_z) \quad (13)$$

Where $\rho$ is fluid density, $A_{Proj}$ is projected area in Z direction, $C_D$ is drag coefficient in wave particular motion direction, $\dot{\phi}_Z$ is velocity of particle motion at Z-direction in complex form and $\dot{X}_z$ is structure velocity at Z-direction

In order to simplify the calculation, the calculation is conducted based on the absolute velocity approach. The floating model dominates term is ignored in the calculation because it is assumed that the fluid particular velocity is much higher compared to structure velocity. Expansion of the equation (13) is shown as follows:

$$\begin{aligned} F_D = {} & \frac{1}{2}\rho A_{Proj} C_D |\dot{\phi}_Z|(\dot{\phi}_Z) - \frac{1}{2}\rho A_{Proj} C_D |\dot{\phi}_Z| \dot{X}_z \\ & - \frac{1}{2}\rho A_{Proj} C_D |\dot{X}_z| \dot{\phi}_Z \\ & + \frac{1}{2}\rho A_{Proj} C_D |\dot{X}_z| \dot{X}_z \end{aligned} \quad (14)$$

By ignoring all the term consist of $|\dot{X}_z|$, equation (14) can be reduced into following format.

$$F_D = \frac{1}{2}\rho A_{Proj} C_D |\dot{\phi}_Z|(\dot{\phi}_Z) - \frac{1}{2}\rho A_{Proj} C_D |\dot{\phi}_Z| \dot{X}_z \quad (15)$$

The above equation (15) is still highly nonlinear and this is impossible to combine with the linear analysis based on diffraction potential theory. To able the drag force to join with the diffraction force calculated with diffraction potential theory, the nonlinear drag term is then expanded in Fourier series. By using the Fourier series linearization method, equation (15) can be written in the linear form as follow:

$$F_D = \frac{1}{2}\rho A_{Proj} C_D \frac{8}{3\pi} V_{max}(\dot{\phi}_Z) - \frac{1}{2}\rho A_{Proj} C_D \frac{8}{3\pi} V_{max} \dot{X}_z \quad (16)$$

Where, $V_{max}$ in equation (16) is the magnitude of complex fluid particle velocity in Z direction. From the equation (16), it can summarize that the first term is linearize drag force due to wave and the second term is the viscous damping force due to the drag effect.

According to Christina Sjöbris, the linearize term $8/3\pi\, V_{max}$ in the equation (16) is the standard result which can be obtained if the work of floating structure performance at resonance is assumed equal between nonlinear and linearized damping term [8].

The linearize drag equation as shown in equation (16) now can be combined with the diffraction term which calculated by diffraction potential theory. The modified motion equation is shown as follows:

$$\begin{aligned} (m + m_a)\ddot{X}_z + \left(b_p + \frac{1}{2}\rho A_{Proj} C_D \frac{8}{3\pi} V_{max}\right)\dot{X}_z + kx \\ = F_p + \frac{1}{2}\rho A_{Proj} C_D \frac{8}{3\pi} V_{max}(\dot{\phi}_Z) \end{aligned} \quad (17)$$

Where $m$ is mass, $k$ is restoring force, $m_a$, $b_p, F_p$ is heave added mass, heave diffraction damping coefficient and heave diffraction force calculated from diffraction potential method respectively. $\frac{1}{2}\rho A_{Proj} C_D \frac{8}{3\pi} V_{max}$ is the viscous damping and $\frac{1}{2}\rho A_{Proj} C_D \frac{8}{3\pi} V_{max}(\dot{\phi}_Z)$ is the drag force based on drag term of Morison equation.

### 2.5 Differentiation of Wave Potential for Morison Drag Force

To obtain the drag force contributed to heave motion, the wave particle velocity at heave direction must be obtained first. This water particle motion is proposed to obtain from the linear wave potential equation. From the theoretical, differential of the wave potential motion in Z-direction will give the speed of water particle motion in the Z-direction.

As mentioned, the drag force in Morison equation is in the function of time; therefore, the time and space dependent wave potential in the complex form should be used here. The wave potential in Euler form as follows:

$$\phi(x,y,z) = \frac{\varsigma g}{w} e^{-Kz + iKR + i\alpha} \quad (18)$$

The expending for the equation (18) obtained that

$$\begin{aligned} \phi(x,y,z) = {} & \frac{\varsigma g}{w} e^{-Kz} \cdot [\cos(KR) + i\sin(KR)] \\ & \cdot [\cos\alpha + i\sin\alpha] \end{aligned} \quad (19)$$

Rearrange the equation (19), the simplify equation as follows

$$\phi(x,y,z) = \frac{\varsigma g}{w} e^{-Kz} \cdot [\cos(KR + \alpha) + i\sin(KR) + \alpha] \quad (20)$$

Differentiate the equation (20) to the Z-direction, the water particle velocity at Z-direction is shown as follows:

$$\begin{aligned} \phi_Z(x,y,z) = {} & \frac{\varsigma g}{w}(-K) e^{-Kz} \\ & \cdot [\cos(KR + \alpha) + i\sin(KR) + \alpha] \end{aligned} \quad (21)$$

Since this numerical model is built for deep water condition, hence it can replace the equation by $Kg = w^2$ and the equation (21) is becoming as follow:

$$\phi_Z(x,y,z) = \varsigma we^{-Kz} \cdot [\cos(KR+\alpha) + i\sin(KR+\alpha)] \quad (22)$$

In the equations (18) to (22), $\varsigma$ is the wave amplitude, $g$ is the gravity acceleration, $w$ is the wave speed, $K$ is wave number, $R$ is the horizontal distance referring to zero coordinate, $\alpha$ is the time dependent variable.

The horizontal distance, $R$ and the time dependent variable, $\alpha$ can be calculated by the following equation

$$R = Kx\cos\beta + Ky\sin\beta \quad (23)$$

$$\alpha = wt + \epsilon \quad (24)$$

In equation (23) and equation (24), the variable $\beta$ is wave heading angle, $\epsilon$ is the leading phase of the wave particle velocity at the Z-direction and $t$ is time.

To calculate the drag forces by using the Morison equation, equation (22) can be modified by following the assumptions below.

First, since the Morison equation is a two dimensional method, therefore the projected area of the Z-direction is all projected at the bottom of structure.

Second, as mentioned in the previous part, this method applies the absolute velocity method and the heave motion of model is considered very small and can be neglected; therefore, the change of displacement in Z-direction is neglected.

From the first and second assumption, the variable $z$ at equation (22) is no effected by time and it is a constant and equal to the draught of the structure. By ignore the time series term, and then the equation (22) can be become as follow:

$$\phi_Z(x,y,z) = \varsigma we^{-Kz} \cdot [\mathrm{Cos}(KR) + i\,\mathrm{Sin}(KR)] \quad (25)$$

### 2.3 Determination of Drag Coefficient

Typically the drag coefficient can be identified from experimental results for more accurate study. In this study, the drag coefficient is determined based on previous empirical data. To able the previous empirical used in this study, the Round Shape FPSO assumed as a vertical cylinder. Second, the laminar flow condition is applied to calculate the drag damping and drag force so it is match with the assumption applied in diffraction potential theory. The drag coefficient applied in the calculation of motion response of Round Shape FPSO as listed in Table 1 and the reference of the dimension used in calculate the drag coefficient is showed in Figure 1.

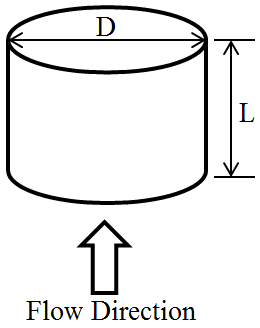


**Figure 1** Dimension of vertical cylinder and flow direction

**Table 1** Drag coefficient for cylinder with the flow direction in vertical direction [10]

| Aspect Ratio, AR $Length, L/Diameter, D$ | Drag Coefficient, $C_D$ |
|---|---|
| 0.5 | 1.1 |
| 1 | 0.9 |
| 2 | 0.9 |
| 4 | 0.9 |
| 8 | 1.0 |

## 3.0 MODELLING RULE

In this study, the FPSO model and mooring lines in model scale are scaling follow the Froude similarity. Froude's law of similarity is the most appropriate scaling law applicable for the free and moored floating structure experiments. The Froude number has a dimension corresponding to the ratio of $u^2/gD$ where $u$ is the fluid velocity, $g$ is the gravity acceleration and $D$ is a length of the model or prototype. The Froude number $Fr$ is defined as $Fr = u^2/gD$.

Let the subscripts $p$ and $m$ stand for prototype and model respectively and $\lambda$ is the scale factor, then the scaling for length, speed, mass and force is shown in Table 2.

**Table 2** Scaling law between model and prototype

| Dimension | Scaling equation |
|---|---|
| **length, $l$ (m)** | $l_p = \lambda l_m$ |
| **speed, $u$ (m/s)** | $u_p = \sqrt{\lambda} u_m$ |
| **mass, m (kg)** | $m_p = \lambda^3 m_m$ |
| **Force, F (N)** | $F_p = 1.025\lambda^3 F_m$ |
| **Mooring line stiffness in water, K (N/m)** | $K_p = 1.025\lambda^2 K_m$ |

## 4.0 WAVE TANK EXPERIMENT

### 4.1 Mooring Selection

In this experiment, four model scale mooring lines attached to the Round Shape FPSO to provide horizontal restoring force to the model. The catenary mooring lines in full scale was designed by using the catenary theory and then scaled down to model scale follow by the scaling rule. The mooring line profile used in this experiment is showed in Figure 2 and the segment particular is showed in Table 3. The size of these mooring lines is pre-determined before the model experiment and the suitability of the mooring lines is analyzed using numerical simulation method to simulation the mooring performance in both static and dynamic condition.

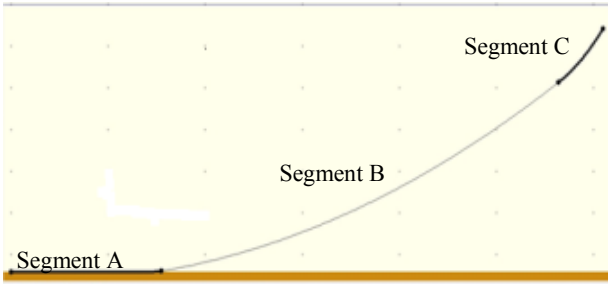


**Figure 2** Mooring line profile

**Table 3** Model catenary mooring line segment information

| Particular | Segment A | Segment B | Segment C |
|---|---|---|---|
| | Model | Model | Model |
| **Nominal Diameter (mm)** | 3.0 | 3.0 | 3.0 |
| **Type** | Chain | Wire Rope | Chain |
| **Segment Length (m)** | 4.0 | 9.4 | 1.4 |
| **Air Weight (kg/m)** | 0.16 | 0.0369 | 0.16 |
| **Water weight in water (kg/m)** Model scale water density: 1000kg/m$^3$ | 0.1425 | 0.03119 | 0.1425 |
| **Breaking Load (KN)** | 10.79 | 5.40 | 10.79 |
| **Modulus Elasticity (GPa)** | 114.59 | 61.00 | 114.59 |

The second mooring lines applied to control the motion of FPSO were prepared based on taut mooring concept. By consider the depth of water tank and the size of model; the model scale mooring lines have the length of 14.5 meters each line. The whole mooring lines attached in this test was made from same material. The segment information of the taut mooring lines applied in the model experiment as in Table 4:

**Table 4** Model taut mooring line segment information

| Particular | In Model Size |
|---|---|
| **Nominal Diameter (mm)** | 3.0 |
| **Type** | Wire Rope |
| **Segment Length (m)** | 14.5 |
| **Air Weight (kg/m)** | 0.0369 |
| **Water weight in water (kg/m)** Model scale water density: 1000kg/m$^3$ | 0.03119 |
| **Breaking Load (KN)** | 5.40 |
| **Modulus Elasticity (GPa)** | 61.00 |

## 4.2 Experimental Setup

This experiment is conducted in wave dynamic tank with the length, wide and depth of 60 m, 25 m and 3.2 m respectively. Before the experiment start, the Round FPSO model was fixed in the middle of tank by four mooring lines which connected between the fairleads located in bottom of FPSO with the anchors which sink into the bottom of tank. Each anchor used in the experiment has the weight of 20 kg in air. The position of the anchors and the arrangement of the mooring lines inside the tank were same for both catenary mooring test and taut mooring test. The mooring arrangements are showed in Figure 3 and the view of FPSO model inside wave dynamic tank after installed with mooring lines is showed in Figure 4.

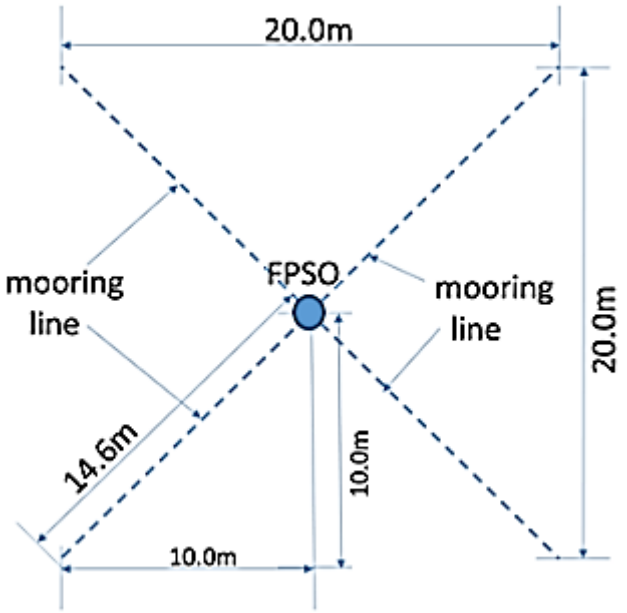


**Figure 3** Arrangement of mooring lines and anchor in wave basin

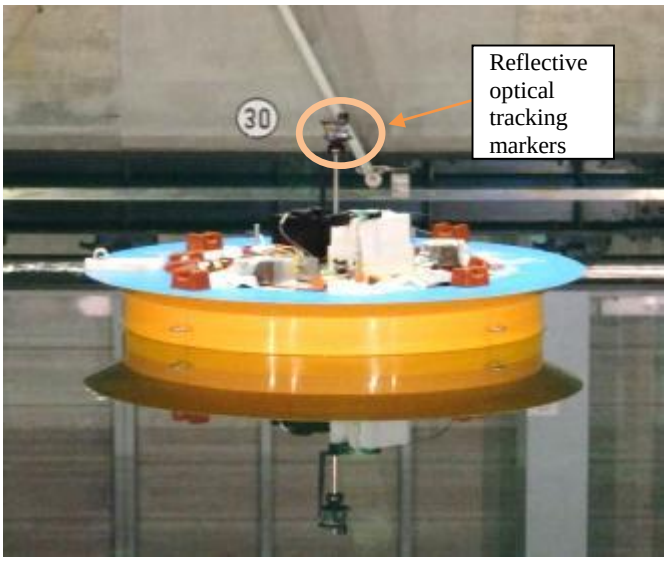


**Figure 4** FPSO model fixed with mooring lines in wave basin in static condition

The round shape FPSO model experienced six degrees of freedom (DoF) during the experiment. The six DoF motions of the FPSO models on model size mooring are measured by theodolite camera system. The theodolite camera able to capture the positions of the reflective optical tracking markers placed on the FPSO model automatically. In this setup, the height of the reflective optical tracking markers is 0.547 m above the vertical center of gravity of the Round Shape FPSO model [6]. The Rotational DoF motions of the FPSO models are measured by gyroscope installed in the center of gravity of the FPSO.

A servo-type wave height measurement device (Servo) was attached to the carriage which located at the position between FPSO model and wave generator to record the wave height generated by the wave generator. To ensure the wave height measure by wave measuring device did not influence by the exist

of Round FPSO, the carriage installed by the servo-type wave height measurement device was moved to the location where the distance between the FPSO to wave measuring device and the distance between wave generator to wave measuring device are 15m both.

All the measurement devices was linked to separate computer to maximize the consistency of the measuring speed. To synchronize the devices and ensure all devices start and stop measure the data without delay, a Wireless remove is used to give an order to start and stop all measurement devices [6].

### 4.3 Linear Motion Data Transformation

As mentioned, the height of the reflective optical tracking markers is 0.547 m above the vertical center of gravity of the Round Shape FPSO model. This also means that the position of the FPSO in wave tank measured by the theodolite camera is not located at the center of gravity of the model. To obtain the exact position of the model referred to model's the center of gravity, the linear motion data must be transferred to the center of gravity of the model. To transfer the data, respective roll, pitch and yaw motion of the model occurred at the same time must be considered in the calculation. The relationships between the positions of the reflective optical tracking markers with the position of center of gravity of model by consider the roll, pitch and yaw motions are showed in Figure 5.

From the Figure 5, $x_p, y_p, z_p$ represent the x, y and z position of the reflective optical tracking markers while $x_G, y_G, z_G$ are the x, y and z position of the center of gravity of model. The relationship between both the position is in the function of length of rod, R, roll angle ($\theta_1$), pitch angle ($\theta_2$), yaw angle ($\theta_3$) and model initial heading angle ($\gamma$). Therefore, the position information at model center of gravity can be calculated as follow:

$$x_g = x_p - \delta x \tag{26}$$

$$y_g = y_p - \delta y \tag{27}$$

$$z_g = z_p - R + \delta z \tag{28}$$

Where, $\delta x, \delta y$ and $\delta z$ can be calculated by following equations

$$\delta z = \left[\frac{R^2}{Tan^2(\theta_1) + Tan^2(\theta_2) + 1}\right]^{1/2} \tag{29}$$

$$\delta r = [R^2 - \delta z^2]^{1/2} \tag{30}$$

$$\alpha = Tan^{-1}\left(\frac{Tan\ \theta_1}{Tan\ \theta_2}\right) \tag{31}$$

$$\delta x = \delta r\ Cos(\theta_3 + \alpha + \gamma) \tag{32}$$

$$\delta y = \delta r\ Sin(\theta_3 + \alpha + \gamma\ ) \tag{33}$$

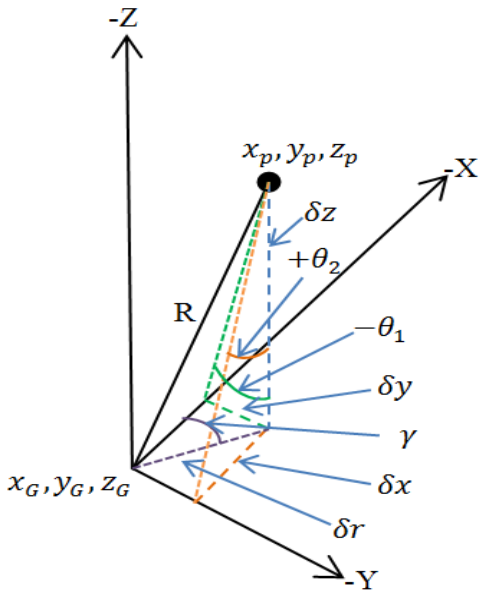


**Figure 5** The relations between the positions of reflective optical tracking markers with position of center of gravity of model

After the position of model referred to its center of gravity is obtained for entire time series, the information can be used to calculate all 6 degree of motions of model. In this experiment setup, the Rotational motions of the FPSO models are measured by gyroscope installed in the models' center of gravity, hence, the measured roll, pitch and yaw motion by the gyroscope are the exact model rotational motions data. However, extra treatment needed for the linear motions which measured by theodolite camera because the time domain position data obtained from the theodolite camera is the model position in the wave tank without consider it direction. By consider the model initial position and initial heading direction, the position data returned from theodolite camera can be used to obtain the model surge, sway and heave motion. In Figure 6, the plan drawing showed the different of global coordinate where these data are measured by theodolite camera and the local coordinate system which required in calculating the linear motion of the FPSO due to the wave.

In Figure 6, X and Y represent the global direction use in the experiment setup while $x$ and $y$ are the local direction where the zero position of local coordinate system located in the model center of gravity before the wave arrived. The model initial heading angle ($\gamma$) was measured from wave progress direction and positive follow clock direction. By reset the zero global coordinates to the model center of gravity at calm sea condition, the 6 DoF motions of the model can be calculated as follow,

$$L = (X^2 + Y^2)^{1/2} \tag{34}$$

$$\beta = Tan^{-1}\frac{Y}{X} \tag{35}$$

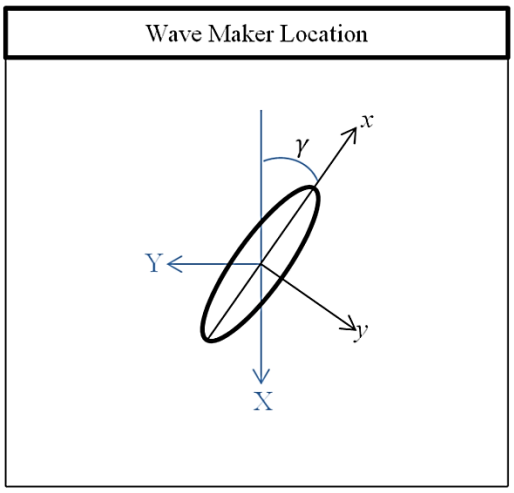


**Figure 6** Plan view of coordinate system

And the six degree freedom of motion for the Round Shape FPSO can be calculated from the Equation (36) to Equation (41).

$$Surge, E_1 = L\ Cos(\beta - \gamma + 180) \quad (36)$$

$$Sway, E_2 = L\ Sin(\beta - \gamma + 180) \quad (37)$$

$$Heave, E_3 = Z_g \quad (38)$$

$$Roll, E_4 = \theta_1 \quad (39)$$

$$Pitch, E_5 = \theta_2 \quad (40)$$

$$Yaw, E_6 = \theta_3 \quad (41)$$

### 4.4 Fourier Series Transformation

The experiment data collected in time series provide the information of wave frequency motion for all 6 degree of motion and slow drift motion at horizontal plan. To split the different motion data, the analysis were conducted in frequency domain where the amplitude of the different types of motion were extracted from the motion amplitude occur at respective frequency.

According to sampling theorem, discretely frequency (Fs) of signal data must be at least twice to the highest continuous signal frequency (F). The continuous signal frequency should discrete by the rate follow the sampling frequency, 1/Fs. Let the discrete sample of the continuous signal have the magnitude of x(k), k=1,2,3,…,n and period between the sample is 1/Fs than a function of a continuous signal, f(t) can be reconstructed back from the discrete sample by the equation below:

$$f(t) = \sum_{k=1}^{k=n} x(k)\ sinc(t \times fs - k) \quad (42)$$

Where,

$$sinc(x) = \frac{\sin(\pi\, x)}{\pi\, x} \quad (43)$$

To convert the data in time domain to the frequency domain, Fast Fourier Transform method was applied in this research. The relationship between function in the time domain, f(t) and frequency domain F(f) is related as the equation below:

$$F(f) = \int_{-\infty}^{\infty} f(t) e^{-j2\pi f(t)} dt \quad (44)$$

Also, for the variable *j*, it represents the square root of (-1) in the natural exponential function.

$$e^{j\theta} = \cos(\theta) + j\ \sin(\theta) \quad (45)$$

Therefore, the discrete data can be written in complex number form as follows:

$$x_i = x(i)_{real} + j\ x(i)_{imaginary} \quad (46)$$

And,

$$x(i)_{real} = \sum_{k=0}^{k=n} X(k) \times \cos\left(\frac{2\pi ki}{n}\right) \quad (47)$$

$$x(i)_{imaginert} = \sum_{k=0}^{k=n} X(k) \times \sin\left(\frac{2\pi ki}{n}\right) \quad (48)$$

And, $i = 2^b$ is the number of data require by Fast Fourier Transform method where b can be any integer number larger than or equal to 1.

Finally, the magnitude, phase and frequency of the signal can be calculated by following equations:

$$X(i)_{magnitude} = \|X(i)\| = \frac{2 \times \sqrt{x(i)_{real}{}^2 + x(i)_{imaginert}{}^2}}{n} \quad (49)$$

$$X(i)_{phase} = tan^{-1}\left[\frac{x(i)_{imaginert}}{x(i)_{real}}\right] \quad (50)$$

$$X(i)_{frequency} = i \times \frac{Fs}{n} \quad (51)$$

## ■5.0 MODEL PARTICULARS

The objective of this research is predicting the wave motion response of new designed Round Shape FPSO and analyse the effect of mooring system to the wave frequency motion response. The designed Round Shape FPSO has the diameter at the draft equal to 111.98 meters and draught of 31.91 meters. The model was constructed from wood following the scale of 1:110

Upon the model complete constructed, inclining test, and roll decay test were conducted to identify the hydrostatic particular of the Round Shape FPSO model. The dimension and measured data of the model were summarized as in Table 5.

**Table 5** Particular of round shape FPSO

| Symbol | Model | Fullscale |
|---|---|---|
| Diameter (m) | 1.018 | 111.98 |
| Depth (m) | 0.4401 | 48.41 |
| Draught (m) | 0.2901 | 31.91 |
| Free board (m) | 0.150 | 16.5 |
| Displacement ($m^3$) | 0.2361 | 314249 |
| Water Plan Area ($m^2$) | 0.8139 | 9848.5 |
| KG (m | 0.2992 | 32.9 |
| GM (m) | 0.069 | 7.6 |

In this study, the numerical method was applied to execute the wave motion response of Round Shape FPSO. The panel method developed based on diffraction potential theory with Morison damping correction as presented at part 2 of this paper require to generate a number of meshes on the model surface in order to predict the distribution of wave force act on this Round FPSO model. To reduce the execution time, symmetry theory is applied in the calculation and total number of panels generated for execution in each symmetry side is 525 (1050 for whole model) for immerse part. The sample of mesh of Round Shape model used in the numerical calculation is shown in Figure 7.

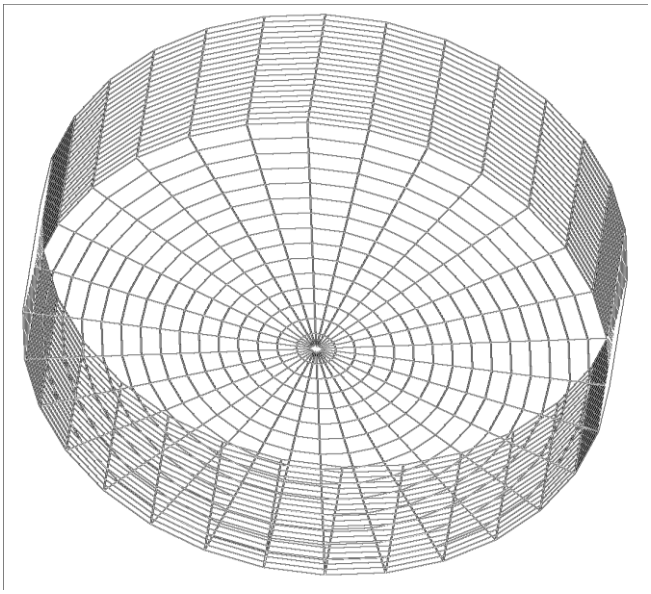

**Figure 7** Meshing for round shape FPSO model

## ■6.0 RESULT AND DISCUSSION

In this paper, the results applied to study the Round FPSO motion response were collected from the numerical simulation and experiment method. The numerical results were generated using ANSYS Hydrodynamic Diffraction software and self-developed programming code based on Diffraction Potential Theory. The experiment results used to study the motion response of the new FPSO were conducted with both the catenary mooring and taut mooring. At the second part of the discussion, the effect of mooring system to the FPSO motion response were analyzed by only using the experiment result. The experiment conducted at same condition but with different mooring system gives the idea of the mooring effect on model wave frequency motion.

### 6.1 Comparison of Numerical and Experimental Simulation

The experiment test is conducted in regular wave condition. In this experiment, the wavelengths were proper selected so it can obtain the tendency of all motions response in response to difference wavelength. In this part, the response amplitude of Round Shape FPSO model in head sea condition was discussed. As shown in Figure 8 to Figure 10, the tendency of surge, pitch and heave motion response obtained by both the numerical and experimental method is agreed between each other. The numerical result predicted that the surge motion tendency experience large change of motion response between the wavelengths 9 meter to 10 meter. However, due to lack of experiment data in this region, the actual condition is difficult to predict. Besides, the experiment and numerical result also showed that the designed FPSO model experience large pitch motion at long wave length region. By compare the pitch and surge response tendency calculated by diffraction potential theory, it is showed that the large change of surge tendency at wavelength from 9 meters to 10 meters may due to the coupling motion of pitch response. The resonance of pitch motion which caused the pitch motion increased significant also influence the surge motion response of this designed model.

Besides, the numerical result also show good agree with experiment result in predict the heave response tendency. Due to involve of the extra viscous damping estimate by the Morison Drag Term in the calculation, the heave response of the Round Shape FPSO model predicted by the numerical method at the damping dominant region did not return a significant over predict error. From the Figure 10, the maximum heave response predicted by the numerical simulation is 1.74 and occurred at wavelength 3.5 meters while the maximum heave response predicted by experiment method is 1.68 and occurred at wavelength 4.5 meters. Comparing the heave response tendency predicted by both the methods, the Figure 10 also shows the numerical result (blue line) is fixed quite well to the heave response data collected from experiment (red dot and green dot). This shows that the developed numerical method which combined the Morison drag term with diffraction potential theory can be applied to predict the heave response of this Round Shape FPSO even in damping dominate region and obtained reasonable accuracy result.

In overall, it observed that the numerical result is able to predict the 6 DOF wave motion response of the Round Shape FPSO in good accuracy if compare to experiment result. Since this designed FPSO model is 4 side symmetry (bow and stern, port-side and starboard side), then the study conducted in the head sea condition is enough to present the motion response characteristic of this model.

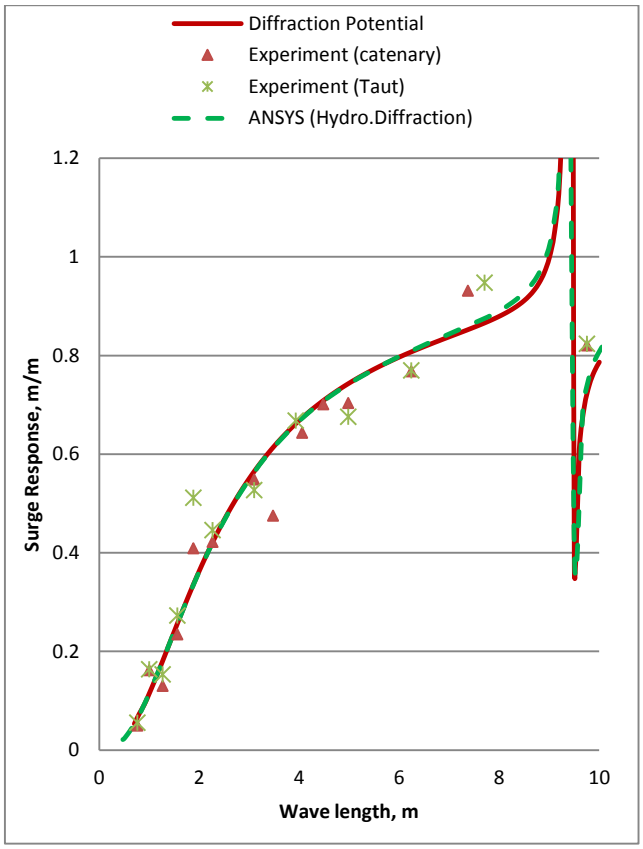


**Figure 8** Surge motion responses of round shape FPSO

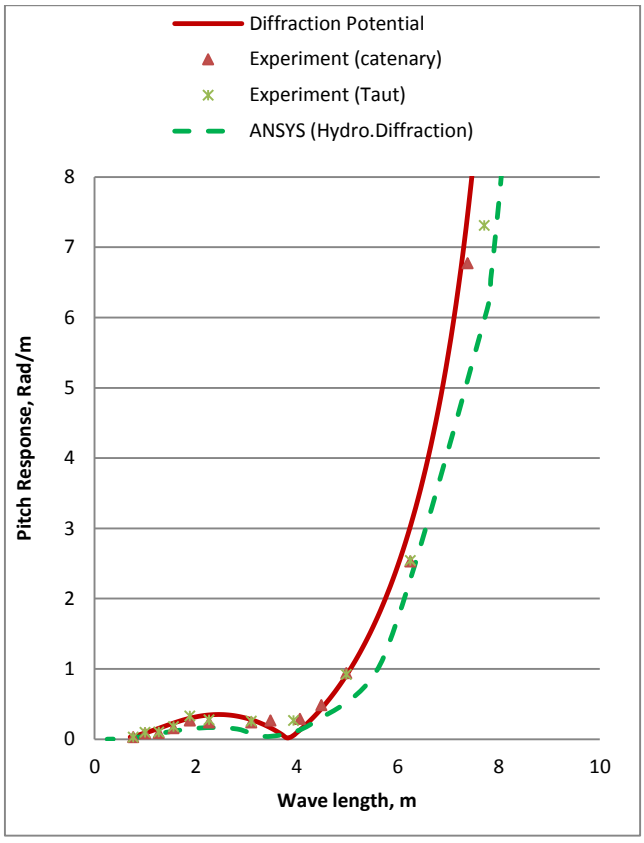


**Figure 9** Pitch motion responses of round shape FPSO

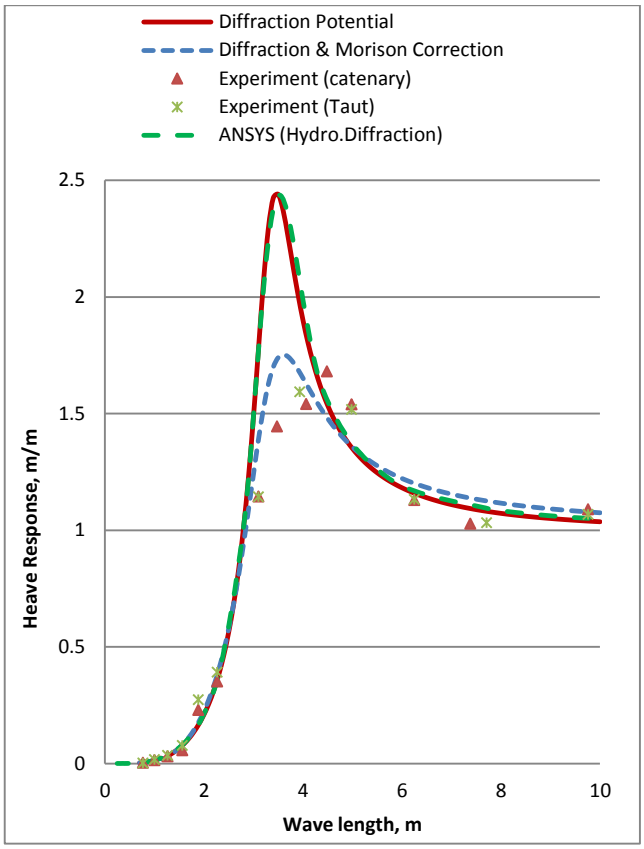


**Figure 10** Heave motion responses of round shape FPSO

### 6.2 Mooring Effect on Round Shape FPSO Wave Response

The result of Round Shape FPSO surge, pitch and heave motion response characteristic predicted by numerical and experiment method are showed in Figure 8 to Figure 10. The motion experiment was conducted to the same model but fixed with different mooring system. In the beginning, the motion experiment was conducted with the Round Shape FPSO model fixed with catenary mooring system. After that the experiment was repeated to the Round FPSO model fixed with the taut mooring system. The experiment results were collected in time series with the sampling rate of 20 data per seconds. To identify the wave frequency motion of the model, the time domain data were converted to the frequency domain using Fourier series transformation method. And then, the motion magnitudes at the wave frequency were identified.

As shows in Figure 8 to Figure 10, the motion experiment results for model fixed with catenary mooring (red dot) and motion experiment results with model fixed with taut mooring (green mark) were plotted verses the wave length. The experiment conducted in the head sea condition, hence only the surge, pitch and heave motion are considered here. By compared the experiment results conducted with the model fixed with different mooring system, it is observed that the magnitude of wave frequency motions detected from the experiment is same for both experiments. Besides, the both set of experiments also show the same tendency with the numerical simulation results. From this observation, the results were shown that the type of mooring setup would not give significant effect to the model motion response if

the wave frequency motion is considered more important than the slow drift motion.

To explain the observation, the numerical results were referred here. The purposed of the mooring applied in the stationary keeping system is control the large offset movement of the floating structure. The movement control by mooring system is the slow drift motion where it is caused by the drift force from wave particle motion. From the numerical study, it is observed that the wave exciting forces act on the model surface are much higher than the drift forces. In this situation, the mooring system which designed to absorb the lower drift forces could not influence much on the wave frequency motion of the model where it is induced by larger wave exciting forces. To highlight this discussion, the surge motion response of the Round Shape FPSO (Figure 8) can be referred as an example here. The surge motion is the horizontal plane motion where the movement on this plane is controlled by the mooring system. However, by comparing the surge RAO of Round Shape FPSO model when it fixed by the catenary mooring and the surge RAO of Round Shape FPSO model when it fixed by the taut mooring, it is showed that both set of the motion responses result collected from the experiments shown the similar tendency and almost similar magnitude of the motion response at any respective wave length. Obviously, the neglect of the mooring forces when study the wave frequency motion is acceptable since the effect is very limited in this type of motion.

## ■7.0 CONCLUSION

The study of the wave frequency motion of Round Shape FPSO was conducted by numerical method and experimental method in this research. Both the numerical and experimental result is agreed between each other for surge, pitch and heave motion of FPSO. To identify the effect of mooring system to the wave frequency motion, the motion experiments were conducted to the same Round FPSO model with two different types of mooring systems. Comparing both set of the experiment results, it is observed that the wave frequency motions responses are almost similar on both set of experiments results. The main reason of this observation also explained by comparing the magnitude of wave exciting force and slow varying drift force. The large difference between both types of forces act on the model caused the effect of mooring system which designed to absorb the slow varying drift forces only able to cause very limited effect to the wave frequency motion. The provided experiment results also showed that the neglect of mooring effect in study the wave frequency motion is possible where it do not show difference between both set of experiment results. Besides, the numerical simulation results which do not consider the mooring effect in the calculation also agreed with both experiments results at any direction of motion and any wavelength.

## References

[1] Lamport, W. B. and Josefsson, P. M. 2008. The Next Generation of Round Fit-for-Purpose Hull form FPSOS Offers Advantages Over Traditional Ship-shaped Hull Forms. 2008 Deep Gulf Conference, December 9–11, New Orleans, Louisiana, USA.

[2] Arslan, T., Pettersen, B. and Andersson, H. I. 2011. *Calculation of the Flow Around Two Interacting Ships*, Computational Methods in Marine Engineering IV, L.Eça, E. Oñate, J. García, T. Kvamsdal and P. Bergan (Eds.). 254–265.

[3] Afrizal, E., Mufti, F. M., Siow, C. L. & Jaswar. 2013. Study of Fluid Flow Characteristic around Rounded-Shape FPSO Using RANS Method. *The 8th International Conference on Numerical Analysis in Engineering*. 46–56. Pekanbaru, Indonesia.

[4] Kvittem, M. I., Bachynski, E. E. & Moan, T. 2012. Effect of Hydrodynamic Modelling in Fully Coupled Simulations of a Semi-Submersible Wind Turbine. *Energy Procedia*. 24.

[5] Koto, J., Siow, C. L., KhairuddinAfrizal, N. M., Abyn, H., Soares, C. G. 2014. Comparison of Floating Structures Motion Prediction Between Diffraction, Diffraction-viscous and Diffraction-Morison Methods. *The 2nd International Conference on Maritime Technology and Engineering*. Lisboa, Portugal.

*[6]* Siow, C. L., Koto, J. Yasukawa, H., Matsuda, A., Terada, D., Soares, C. G., Zameri, M. 2014. Experiment Study on Hydrodynamics Characteristic of Rounded- Shape FPSO. *The 1st Conference on Ocean, Mechanical and Aerospace-Science and Engineering*-Pekanbaru, Indonesia.

[7] Siow, C. L., Koto, J, and Khairuddin, N. M. 2014. Study on Model Scale Rounded-Shape FPSO's Mooring Lines. *Journal of Ocean, Mechanical and Aerospace Science and Engineering*. 12.

[8] Christina Sjöbris. 2012. Decommissioning of SPM Buoy. Master of Science Thesis. Chalmers University of Technology, Gothenburg, Sweden.

[9] Siow, C. L., Koto, J, Yasukawa, H., Matsuda, A., Terada, D., Soares, C. G. 2015. Theoretical Review on Prediction of Motion Response using Diffraction Potential and Morison. *Journal of Ocean, Mechanical and Aerospace Science and Engineering*. 12.

[10] Cengel, Y. A, Cimbala, J. M. 2010. *Fluid Mechanics Fundamentals and Application*. 2nd Ed.